In-plane electronic anisotropy resulted from ordered magnetic moment in iron-based superconductors

S.-F. Wu,[1,*] W.-L. Zhang,[1,†] V. K. Thorsmølle,[1] G. F. Chen,[2] G. T. Tan,[3] P. C. Dai,[4] Y. G. Shi,[2] C. Q. Jin,[2] T. Shibauchi,[5] S. Kasahara,[6] Y. Matsuda,[6] A. S. Sefat,[7] H. Ding,[2] P. Richard,[8] and G. Blumberg[1,9,‡]

[1]*Department of Physics and Astronomy, Rutgers University, Piscataway, New Jersey 08854, USA.*
[2]*Beijing National Laboratory for Condensed Matter Physics, and Institute of Physics, Chinese Academy of Sciences, Beijing 100190, China*
[3]*Center for Advanced Quantum Studies and Department of Physics, Beijing Normal University, Beijing 100875, China*
[4]*Department of Physics and Astronomy, Rice University, Houston, Texas 77005, USA*
[5]*Department of Advanced Materials Science, University of Tokyo, Kashiwa, Chiba 277-8561, Japan*
[6]*Department of Physics, Kyoto University, Sakyo-ku, Kyoto 606-8502, Japan*
[7]*Materials Science & Technology Division, Oak Ridge National Laboratory, Oak Ridge, Tennessee 37831, USA*
[8]*Institut quantique, Université de Sherbrooke, 2500 Boulevard de l'Université, Sherbrooke, Québec J1K 2R1, Canada*
[9]*National Institute of Chemical Physics and Biophysics, 12618 Tallinn, Estonia*

(Received 5 December 2017; revised 30 June 2020; accepted 7 July 2020; published 24 July 2020)

We study the in-plane electronic anisotropy in the parent compounds of several families of Fe-based superconductors ($BaFe_2As_2$, $EuFe_2As_2$, NaFeAs, LiFeAs, FeSe, and LaFeAsO) by polarization-resolved Raman scattering. We measure intensity of the fully symmetric c-axis vibration of As atom mode in the XY scattering geometry and notice that the mode's intensity is significantly enhanced below the magnetostructural transition only for compounds showing magnetic ordering. In particular, we find that the intensity ratio of this As phonon in the XY vs. XX scattering geometries is proportional to the square of the ordered magnetic moment. We relate this As phonon intensity enhancement below the Néel temperature in iron pnictides to in-plane electronic anisotropy induced by the collinear spin-density wave order.

DOI: 10.1103/PhysRevResearch.2.033140

The lattice, orbital, and magnetic degrees of freedom are strongly coupled in the Fe-based superconductors. This is best evidenced by the observation, in most parent compounds, of a magnetic transition from paramagnetic to collinear antiferromagnetic (AFM), occurring at a temperature T_N slightly below the temperature T_S at which a structural transition from tetragonal to orthorhombic phase occurs. The interplay between these degrees of freedom is complex and led to a chicken-egg problem for which there is still no consensual view [1,2]. The electronic structure is directly affected by an electronic band folding accompanied by the formation of a collinear spin-density wave (SDW) gap [3–6]. As a result, a significant electronic anisotropy was found for properties measured along the two planar orthogonal Fe-Fe directions (Fig. 1) below the magnetostructural transition, notably in electrical transport [7], optical conductivity [8,9], thermopower [10], local density-of-states (DOS) imaging [11], and quasiparticle band dispersions [12].

Raman scattering offers a unique way to study the electronic anisotropy below the magnetostructural transition of the iron-based superconductors [6,13]. For example, one can study the interband transitions along the two planar orthogonal Fe-Fe directions (Fig. 1) in a detwinned sample [6] or investigate the As fully symmetric phonon in a twinned sample [14].

In relation to this study, it has been noticed that the Raman coupling vertex to the As fully symmetric phonon: the c-axis vibration of As atom, which modulates the Fe-As-Fe bond angle of the Fe-As tetrahedra (Fig. 1), - is forbidden for XY scattering geometry in the tetragonal phase, whereas the coupling becomes finite in the orthorhombic phase. However, because orthorhombicity of the lattice constants δ for all studied materials is weak, the emerging As mode's intensity due to geometrical lattice anisotropy is expected to be small. Surprisingly, a significant intensity of the As phonon in the nearly forbidden XY scattering geometry has been observed for $Ba(Fe_{1-x}Au_x)_2As_2$ below T_N, in contrast to the weak signals at temperatures between T_S and T_N [14]. Similar results were reported for $Ba(Fe_{1-x}Co_x)_2As_2$ [15]. In addition, the temperature dependence of integrated As phonon intensity was reported to be proportional to square of the magnetic moment $M(T)^2$ below T_N [14]. The origin of this anomalous intensity enhancement was related to the in-plane electronic anisotropy induced by the collinear SDW order

*sw666@physics.rutgers.edu
†Present address: Department of Engineering and Applied Sciences, Sophia University, 7-1 Kioi-cho, Chiyoda-ku, Tokyo 102-8554, Japan.
‡girsh@physics.rutgers.edu

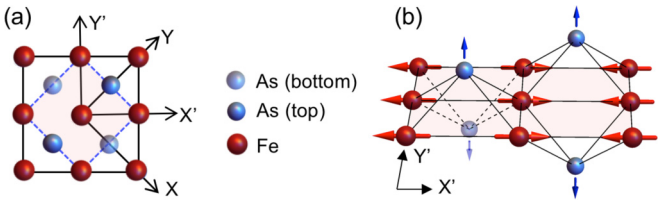

FIG. 1. (a) Definition of the crystallographic directions in the tetragonal 2-Fe unit cell above T_S (light red shaded area) and 4-Fe orthorhombic magnetic unit cell below T_N (black solid lines). (b) Schematic diagram of the magnetic structure. Red arrows: Fe local moments forming collinear AFM order. Blue arrows: c-axes vibrations of the fully symmetric As phonon mode.

[14]. Furthermore, the Fano model analysis of data revealed that temperature dependence of the Raman vertex amplitude is proportional to magnitude of the magnetic order parameter $M(T)$ [14]. While previous Raman study established the intimate link between the As phonon intensity, the electronic anisotropy and the magnetic order parameter by studying the temperature and doping dependence of the As phonon in the 122 system [14], a detailed study of this relation among different families of iron-based superconductors where the ordered magnetic moment varies is still lacking.

In this paper, we employ polarization resolved Raman scattering spectroscopy to study the in-plane electronic anisotropy for typical 122, 111, 1111, and 11 families of Fe-based superconductors. For all compounds showing magnetic ordering, we observe a strong intensity for the fully symmetric As mode appearing below T_N in the nearly forbidden XY scattering channel as a result of significantly enhanced anisotropy of the in-plane electronic polarizability, while no such enhancement is found for compounds without magnetically ordered state. We also find that the ratio of the As phonon intensity in the XY vs. XX scattering geometries, I_{XY}/I_{XX}, is proportional to the square of the magnetic ordered moment M^2. This conclusion is consistent with previous study for $Ba(Fe_{1-x}Au_x)_2As_2$ alloys [14]. Because the geometrical lattice anisotropy $\delta = (a-b)/(a+b)$ below T_S is relatively small, we conclude that the intensity enhancement of the As phonon in the magnetic phase originates from the collinear SDW order-induced in-plane electronic anisotropy.

Single crystals of materials listed in Table I were grown as described in Refs. [16–21]. The corresponding structural phase transition temperature (T_S) and magnetic phase transition temperature (T_N) are summarized in Table I. Raman measurements on $BaFe_2As_2$, NaFeAs, $EuFe_2As_2$, LiFeAs, FeSe were performed using the spectrometer described in Refs. [14]. The measurements of LaFeAsO were performed in a back-scattering geometry using a T64000 triple-stage spectrometer.

TABLE I. Summary of T_S, T_N (in Kelvin), lattice orthorhombicity [$\delta = (a-b)/(a+b)$], intensity ratio of A_g phonon in XY vs. XX geometries, and ordered magnetic moment/Fe M (in μ_B) for compounds studied in this paper.

Sample	T_S/T_N	δ (%)	I_{XY}/I_{XX}	M
$EuFe_2As_2$ [16]	175/175	0.5 [22]	3.3	0.98 [23]
$BaFe_2As_2$ [16]	135/135	0.4 [24]	3.1	0.87 [25]
LaFeAsO [19,20]	155/137	0.24 [20]	0.54	0.36-0.6 [25]
NaFeAs [18]	55/40	0.18 [26]	0.16	0.09 [25]
FeSe [21]	90/–	0.25 [27]	0.017	–
LiFeAs [28]	–/–	0	0	–

The phononic Raman scattering intensity is proportional to $I \propto |\hat{e}_i \cdot \mathbf{R} \cdot \hat{e}_s|^2$, where $\hat{e}_i$ and $\hat{e}_s$ are the polarization unit vectors of the incoming and scattering light, respectively, and $\mathbf{R}$ is the Raman tensor [29]. For the D_{4h} point group the XX, XY, $X'X'$, and $X'Y'$ polarization geometries probe $A_{1g}+B_{1g}$, $A_{2g}+B_{2g}$, $A_{1g}+B_{2g}$, and $A_{2g}+B_{1g}$ symmetry excitations, respectively. In the orthorhombic phase with D_{2h} point group symmetry, the unit cell rotates by 45°; the A_{1g} and B_{2g} representations of the D_{4h} point group merge into the A_g representation of the D_{2h} point group, and A_{2g} and B_{1g} (D_{4h}) merge into B_{1g} (D_{2h}). In the orthorhombic phase, the XX and XY polarization geometries probe A_g+B_{1g} and A_g symmetry excitations, respectively [14].

Before investigating the behavior of the A_{1g}/A_g symmetry As phonon across the magnetostructural transitions, we first examine the A_{1g} and A_g Raman tensors:

$$A_{1g}^{D_{4h}} = \begin{pmatrix} \bar{a} & 0 & 0 \\ 0 & \bar{a} & 0 \\ 0 & 0 & \bar{c} \end{pmatrix}, \quad A_g^{D_{2h}} = \begin{pmatrix} \frac{(\bar{a}'+\bar{b}')}{2} & \frac{(\bar{a}'-\bar{b}')}{2} & 0 \\ \frac{(\bar{a}'-\bar{b}')}{2} & \frac{(\bar{a}'+\bar{b}')}{2} & 0 \\ 0 & 0 & \bar{c} \end{pmatrix},$$

where $A_g^{D_{2h}}$ (orthorhombic phase) has been rotated by 45° to keep the same XYZ axis notation as in the tetragonal phase. Here, $\bar{a}'$ and $\bar{b}'$ are the diagonal elements of the $A_g^{D_{2h}}$ Raman tensor in the natural coordinate system of the orthorhombic phase (before the 45° rotation).

Accordingly, the A_{1g}-symmetry mode is forbidden in the XY scattering geometry in the tetragonal phase. This is the case for LiFeAs, which shows neither structural nor magnetic transition. As shown in Fig. 2(a), sharp Raman phonon peaks at 186 cm^{-1} and 237 cm^{-1}, corresponding to a A_{1g}(As) and a B_{1g}(Fe) modes, respectively, are detected in the XX scattering geometry. However, as expected for the tetragonal structure of LiFeAs, these modes have no intensity in the XY scattering geometry. Similar Raman results are reported for the tetragonal $Fe_{1+y}Te_{0.6}Se_{0.4}$ single crystal [30].

If anisotropy develops in the orthorhombic phase, the A_g anion mode may acquire a finite intensity $|(\bar{a}'-\bar{b}')/2|^2$ in the XY scattering geometry related to the anisotropy of the in-plane polarizability associated to this A_g anion mode, because $\bar{a}'$ and $\bar{b}'$ are the polarizability derivatives along the two Fe-Fe orthogonal directions (X' and Y') in the orthorhombic phase. Since the lattice orthorhombicity δ is small (Table I), the intensity due to geometrical anisotropy is expected to be weak. For example, for the FeSe material, which exhibits a structural phase transition at 90 K [31,32] but no long-range magnetic ordering, we observe a A_g(Se) phonon at 180 cm^{-1} and a B_{1g}(Fe) phonon at 208 cm^{-1} for the XX polarization [Fig. 2(b)]. Although the intensity of the A_g(Se) phonon with the XY polarization is finite at 20 K [inset of Fig. 2(b)], it is only 2% of the corresponding intensity recorded for the XX polarization (Table I) [13,33].

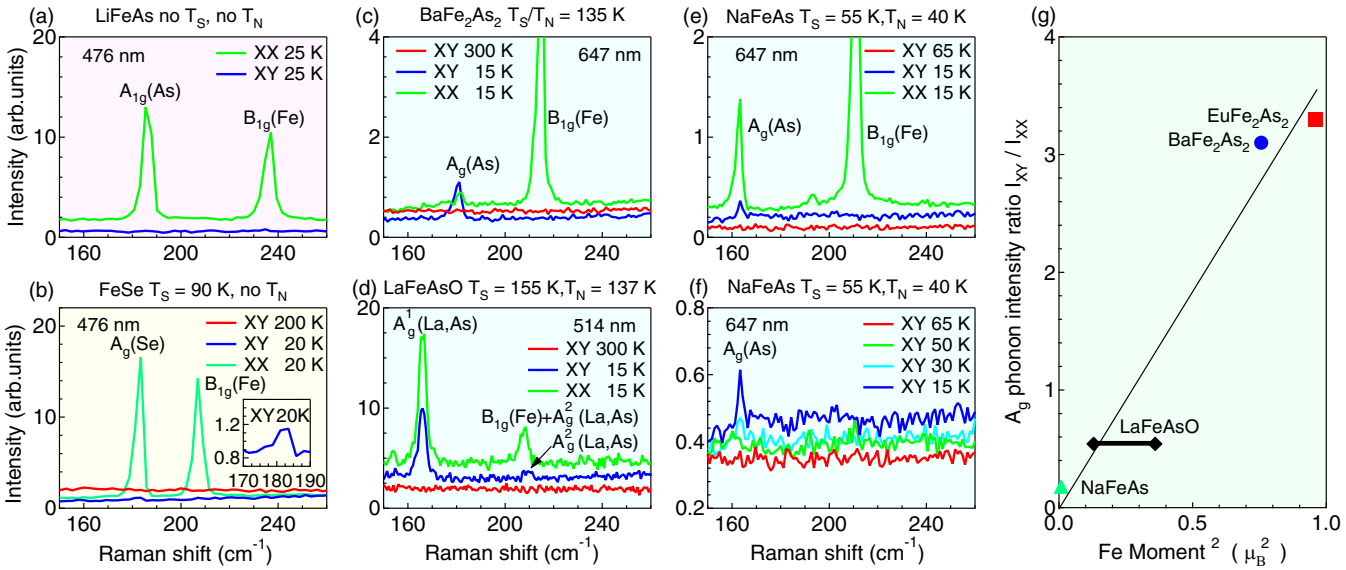

FIG. 2. Comparison of Raman spectra (shifted for clarity) in XX and XY scattering geometries for different parent compounds: (a) LiFeAs, (b) FeSe, (c) $BaFe_2As_2$, (d) LaFeAsO, (e) and (f) NaFeAs. When finite, the T_N and T_S values are indicated on the top of the corresponding panel. (g) A_g(As) phonon intensity ratio in XY vs. XX geometries (I_{XY}/I_{XX}) at 15 K as a function of the squared ordered magnetic moment/Fe [23,25]. The black line is a linear fit.

In contrast, $BaFe_2As_2$ with strong magnetic ordering clearly shows the 181 cm^{-1} A_g (As) mode [13,15,34,35] in the XY scattering geometry below T_N [Fig. 2(c)]. Similar observation is made for NaFeAs [Figs. 2(e) and 2(f)], which also encounters both a structural and a magnetic phase transition: (i) We observe only a weak intensity between T_S and T_N, and (ii) the 162 cm^{-1} A_g(As) phonon mode appears in the XY spectra only below T_N. LaFeAsO [36–38] is another system with split structural and magnetic phase transitions. In this case as well, we detect sizable intensity for the A_g^1 (in-phase La and As) mode at 166 cm^{-1} and the A_g^2 (out-of-phase La and As) mode at 209 cm^{-1} in the XY scattering geometry below T_N [Fig. 2(d)].

To quantify the intensity of the A_g(As) phonon in the XY scattering geometry below T_N in different families of Fe-based superconductors, we study the ratio between the A_g(As) mode intensity in the XY and XX scattering geometries I_{XY}/I_{XX}. This ratio is proportional to $|(\bar{a}' - \bar{b}')/(\bar{a}' + \bar{b}')|^2$, which is a direct measure of the in-plane polarizability anisotropy of the A_g(As) mode. Based on Table I, the ratio I_{XY}/I_{XX} is significant only for compounds with long-range magnetic ordering. For example, the ratio I_{XY}/I_{XX} is 300% for $BaFe_2As_2$, 16% for NaFeAs and 50% for LaFeAsO, as compared to 2% for FeSe, i.e., 1–2 orders of magnitude smaller. Such behavior cannot be solely explained by weak geometrical lattice orthorhombicity δ, instead, the observation relates the mode's intensity to magnetic order parameter. This is best evident from Fig. 2(g), where we show that the I_{XY}/I_{XX} ratio of the A_g(As) phonon intensity for different Fe-based families is proportional to the square of the magnetic moment M^2.

In conclusion, we revealed a significant intensity enhancement of the emergent A_g(As) phonon mode in the XY scattering geometry below T_N only for parent compounds of Fe-based superconductors showing magnetic order. We demonstrate that the ratio of the As phonon intensity in the XY and XX scattering geometries I_{XY}/I_{XX} is proportional to the square of the magnetic ordered moment M^2. We conclude that the generic A_g(As) phonon intensity enhancement below T_N in iron pnictides is due to the in-plane electronic anisotropy induced by the collinear SDW order: a larger ordered moment in the magnetic phase results in lager in-plane electronic anisotropy, which in turn cause larger As phonon intensity ratio I_{XY}/I_{XX} below T_N.

We thank E. Bascones and K. Haule for discussions. The spectroscopic work conducted at Rutgers (S.-F.W., W.-L.Z., V.K.T., and G.B.) was supported by NSF Grant No. DMR-1709161. The sample preparation and characterization at ORNL (A.S.S.) was supported by the US Department of Energy, Basic Energy Sciences, Materials Sciences and Engineering Division. The work at NICPB was supported by the Estonian Research Council Grant No. PRG736 and by the European Research Council (ERC) under Grant Agreement No. 885413.

[1] R. M. Fernandes, A. V. Chubukov, and J. Schmalian, What drives nematic order in iron-based superconductors? Nature Phys. **10**, 97 (2014).

[2] R. M. Fernandes, L. H. VanBebber, S. Bhattacharya, P. Chandra, V. Keppens, D. Mandrus, M. A. McGuire, B. C. Sales, A. S. Sefat, and J. Schmalian, Effects of Nematic Fluctuations

on the Elastic Properties of Iron Arsenide Superconductors, Phys. Rev. Lett. **105**, 157003 (2010).

[3] W. Z. Hu, J. Dong, G. Li, Z. Li, P. Zheng, G. F. Chen, J. L. Luo, and N. L. Wang, Origin of the Spin Density Wave Instability in AFe_2As_2 (A=Ba,Sr) as Revealed by Optical Spectroscopy, Phys. Rev. Lett. **101**, 257005 (2008).

[4] Y. Ran, F. Wang, H. Zhai, A. Vishwanath and D.-H. Lee, Nodal spin density wave and band topology of the FeAs-based materials, Phys. Rev. B **79**, 014505 (2009).

[5] P. Richard, K. Nakayama, T. Sato, M. Neupane, Y.-M. Xu, J. H. Bowen, G. F. Chen, J. L. Luo, N. L. Wang, X. Dai, Z. Fang, H. Ding and T. Takahashi, Observation of Dirac Cone Electronic Dispersion in $BaFe_2As_2$, Phys. Rev. Lett. **104**, 137001 (2010).

[6] W.-L. Zhang, Z. P. Yin, A. Ignatov, Z. Bukowski, Janusz Karpinski, Athena S. Sefat, H. Ding, P. Richard, and G. Blumberg, Raman scattering study of spin-density-wave-induced anisotropic electronic properties in AFe_2As_2 (A=Ca, Eu), Phys. Rev. B **93**, 205106 (2016).

[7] J.-H. Chu, J. G. Analytis, K. De Greve, P. L. McMahon, Z. Islam, Y. Yamamoto, and I. R. Fisher, In-plane resistivity anisotropy in an underdoped iron arsenide superconductor, Science **329**, 824 (2010).

[8] A. Dusza, A. Lucarelli, F. Pfuner, J.-H. Chu, I. R. Fisher, and L. Degiorgi, Anisotropic charge dynamics in detwinned $Ba(Fe_{1-x}Co_x)_2As_2$, Europhys. Lett. **93**, 37002 (2011).

[9] M. Nakajima, T. Liang, S. Ishida, Y. Tomioka, K. Kihou, C. H. Lee, A. Iyo, H. Eisaki, T. Kakeshita, T. Ito, and S. Uchida, Unprecedented anisotropic metallic state in undoped iron arsenide $BaFe_2As_2$ revealed by optical spectroscopy, Proc. Natl. Acad. Sci. USA **108**, 12238 (2011).

[10] S. Jiang, H. S. Jeevan, J. K. Dong, and P. Gegenwart, Thermopower As a Sensitive Probe of Electronic Nematicity in Iron Pnictides, Phys. Rev. Lett. **110**, 067001 (2013).

[11] E. P. Rosenthal, E. F. Andrade, C. J. Arguello, R. M. Fernandes, L. Y. Xing, X. C. Wang, C. Q. Jin, A. J. Millis, and A. N. Pasupathy, Visualization of electron nematicity and unidirectional antiferroic fluctuations at high temperatures in NaFeAs, Nature Phys. **10**, 225 (2014).

[12] M. Yi, D. Lu, J.-H. Chu, J. G. Analytis, A. P. Sorini, A. F. Kemper, B. Moritz, S.-K. Mo, R. G. Moore, M. Hashimoto, W.-S. Lee, Z. Hussain, T. P. Devereaux, I. R. Fisher, and Z.-X. Shen, Symmetry-breaking orbital anisotropy observed for detwinned $Ba(Fe_{1-x}Co_x)_2As_2$ above the spin density wave transition, Proc. Natl. Acad. Sci. USA **108**, 6878 (2011).

[13] A. Baum, Y. Li, M. Tomić, N. Lazarević, D. Jost, F. Löffler, B. Muschler, T. Böhm, J.-H. Chu, I. R. Fisher, R. Valentí, I. I. Mazin, and R. Hackl, Interplay of lattice, electronic, and spin degrees of freedom in detwinned $BaFe_2As_2$: A Raman scattering study, Phys. Rev. B **98**, 075113 (2018).

[14] S.-F. Wu, W.-L. Zhang, L. Li, H.-B. Cao, H.-H. Kung, A. S. Sefat, H. Ding, P. Richard, and G. Blumberg, Coupling of fully symmetric As phonon to magnetism in $Ba(Fe_{1-x}Au_x)_2As_2$, Phys. Rev. B **102**, 014501 (2020).

[15] F. Kretzschmar, T. Bohm, U. Karahasanovic, B. Muschler, A. Baum, D. Jost, J. Schmalian, S. Caprara, M. Grilli, C. Di Castro, J. G. Analytis, J.-H. Chu, I. R. Fisher, and R. Hackl, Critical spin fluctuations and the origin of nematic order in $Ba(Fe_{1-x}Co_x)_2As_2$, Nature Phys. **12**, 560 (2016).

[16] A. S. Sefat, Bulk synthesis of iron-based superconductors, Curr. Opin. Solid State Mater. Sci. **17**, 59 (2013).

[17] L. Li, H. B. Cao, M. A. McGuire, J. S. Kim, G. R. Stewart, and A. S. Sefat, Role of magnetism in superconductivity of $BaFe_2As_2$: Study of 5*d* Au-doped crystals, Phys. Rev. B **92**, 094504 (2015).

[18] M. A. Tanatar, N. Spyrison, K. Cho, E. C. Blomberg, G. Tan, P. Dai, C. Zhang, and R. Prozorov, Evolution of normal and superconducting properties of single crystals of $Na_{1-\delta}FeAs$ upon interaction with environment, Phys. Rev. B **85**, 014510 (2012).

[19] Y. Kamihara, T. Watanabe, M. Hirano, and H. Hosono, Iron-based layered superconductor $LaO_{1-x}F_xFeAs$ ($x = 0.05 - 0.12$) with $T_c = 26$ K, J. Am. Chem. Soc **130**, 3296 (2008).

[20] C. de la Cruz, Q. Huang, J. W. Lynn, J. Li, W. R. II, J. L. Zarestky, H. A. Mook, G. F. Chen, J. L. Luo, N. L. Wang, and P. C Dai, Magnetic order close to superconductivity in the iron-based layered $LaO_{1-x}F_xFeAs$ systems, Nature (London) **453**, 899 (2008).

[21] S. Hosoi, K. Matsuura, K. Ishida, H. Wang, Y. Mizukami, T. Watashige, S. Kasahara, Y. Matsuda, and T. Shibauchi, Nematic quantum critical point without magnetism in $FeSe_{1-x}S_x$ superconductors, Proc. Natl. Acad. Sci. USA **113**, 8139 (2016).

[22] M. Tegel, M. Rotter, V. Weiß, F. M. Schappacher, R. Pöttgen, and D. Johrendt, Structural and magnetic phase transitions in the ternary iron arsenides $SrFe_2As_2$ and $EuFe_2As_2$, J. Phys.: Condens. Matter **20**, 452201 (2008).

[23] Y. Xiao, Y. Su, M. Meven, R. Mittal, C. M. N. Kumar, T. Chatterji, S. Price, J. Persson, N. Kumar, S. K. Dhar, A. Thamizhavel, and Th. Brueckel, Magnetic structure of $EuFe_2As_2$ determined by single-crystal neutron diffraction, Phys. Rev. B **80**, 174424 (2009).

[24] Q. Huang, Y. Qiu, W. Bao, M. A. Green, J. W. Lynn, Y. C. Gasparovic, T. Wu, G. Wu, and X. H. Chen, Neutron-Diffraction Measurements of Magnetic Order and a Structural Transition in the Parent $BaFe_2As_2$ Compound of FeAs-Based High-Temperature Superconductors, Phys. Rev. Lett. **101**, 257003 (2008).

[25] P. C. Dai, Antiferromagnetic order and spin dynamics in iron-based superconductors, Rev. Mod. Phys. **87**, 855 (2015).

[26] S. Li, C. de la Cruz, Q. Huang, G. F. Chen, T.-L. Xia, J. L. Luo, N. L. Wang, and P. C Dai, Structural and magnetic phase transitions in $Na_{1-\delta}FeAs$, Phys. Rev. B **80**, 020504(R) (2009).

[27] T. M. McQueen, A. J. Williams, P. W. Stephens, J. Tao, Y. Zhu, V. Ksenofontov, F. Casper, C. Felser, and R. J. Cava, Tetragonal-to-Orthorhombic Structural Phase Transition at 90 K in the Superconductor $Fe_{1.01}Se$, Phys. Rev. Lett. **103**, 057002 (2009).

[28] X. C. Wang, Q. Q. Liu, Y. X. Lv, Z. Deng, K. Zhao, R. C. Yu, J. L. Zhu, and C. Q Jin, Superconducting properties of "111" type LiFeAs iron arsenide single crystals, Sci. China Phys. Mech. **53**, 1199 (2010).

[29] M. V. Klein, Electronic Raman Scattering, in *Light Scattering in Solids I*, Vol. 8, edited by M. Cardona (Springer-Verlag, Berlin, 1983), Chap. 4, pp. 147–202.

[30] S.-F. Wu, A. Almoalem, I. Feldman, A. Lee, A. Kanigel, and G. Blumberg, Superconductivity and phonon self-energy effects in $Fe_{1+y}Te_{0.6}Se_{0.4}$, Phys. Rev. Research **2**, 013373 (2020).

[31] A. E. Böhmer, F. Hardy, F. Eilers, D. Ernst, P. Adelmann, P. Schweiss, T. Wolf, and C. Meingast, Lack of coupling between superconductivity and orthorhombic distortion in stoichiometric single-crystalline FeSe, Phys. Rev. B **87**, 180505(R) (2013).

[32] A. E. Böhmer, T. Arai, F. Hardy, T. Hattori, T. Iye, T. Wolf, H. v. Löhneysen, K. Ishida, and C. Meingast, Origin of the Tetragonal-to-Orthorhombic Phase Transition in FeSe: A Combined Thermodynamic and NMR Study of Nematicity, Phys. Rev. Lett. **114**, 027001 (2015).

[33] W.-L. Zhang, S.-F. Wu, S. Kasahara, T. Shibauchi, Y. Matsuda, and G. Blumberg, arXiv:1710.09892.

[34] L. Chauvière, Y. Gallais, M. Cazayous, A. Sacuto, M. A. Méasson, D. Colson, and A. Forget, Doping dependence of the lattice dynamics in $Ba(Fe_{1-x}Co_x)_2As_2$ studied by Raman spectroscopy, Phys. Rev. B **80**, 094504 (2009).

[35] S. Sugai, Y. Mizuno, R. Watanabe, T. Kawaguchi, K. Takenaka, H. Ikuta, Y. Takayanagi, N. Hayamizu, and Y. Sone, Spin-density-wave gap with dirac nodes and two-magnon Raman scattering in $BaFe_2As_2$, J. Phys. Soc. Jpn. **81**, 024718 (2012).

[36] U. F. Kaneko, P. F. Gomes, A. F. García-Flores, J.-Q. Yan, T. A. Lograsso, G. E. Barberis, D. Vaknin, and E. Granado, Nematic fluctuations and phase transitions in LaFeAsO: A Raman scattering study, Phys. Rev. B **96**, 014506 (2017).

[37] V. G. Hadjiev, M. N. Iliev, K. Sasmal, Y.-Y. Sun, and C. W. Chu, Raman spectroscopy of *R*FeAsO (*R*=Sm, La), Phys. Rev. B **77**, 220505(R) (2008).

[38] S. C. Zhao, D. Hou, Y. Wu, T. L. Xia, A. M. Zhang, G. F. Chen, J. L. Luo, N. L. Wang, J. H. Wei, Z. Y. Lu, and Q. M. Zhang, Raman spectra in iron-based quaternary $CeO_{1-x}F_xFeAs$ and $LaO_{1-x}F_xFeAs$, Supercond. Sci. Tech **22**, 015017 (2008).